THE JOURNAL OF PHYSICAL CHEMISTRY Letters

Letter

pubs.acs.org/JPCL

Molecular-structure Control of Ultrafast Electron Injection at Cationic Porphyrin−CdTe Quantum Dot Interfaces

Shawkat M. Aly,† Ghada H. Ahmed, Basamat S. Shaheen, Jingya Sun, and Omar F. Mohammed*

Solar and Photovoltaics Engineering Research Center, Division of Physical Sciences and Engineering, King Abdullah University of Science and Technology (KAUST), Thuwal 23955-6900, Kingdom of Saudi Arabia

Supporting Information

ABSTRACT: Charge transfer (CT) at donor (D)/acceptor (A) interfaces is central to the functioning of photovoltaic and light-emitting devices. Understanding and controlling this process on the molecular level has been proven to be crucial for optimizing the performance of many energy-challenge relevant devices. Here, we report the experimental observations of controlled on/off ultrafast electron transfer (ET) at cationic porphyrin−CdTe quantum dot (QD) interfaces using femto- and nanosecond broad-band transient absorption (TA) spectroscopy. The time-resolved data demonstrate how one can turn on/off the electron injection from porphyrin to the CdTe QDs. With careful control of the molecular structure, we are able to tune the electron injection at the porphyrin−CdTe QD interface from zero to very efficient and ultrafast. In addition, our data demonstrate that the ET process occurs within our temporal resolution of 120 fs, which is one of the fastest times recorded for organic photovoltaics.

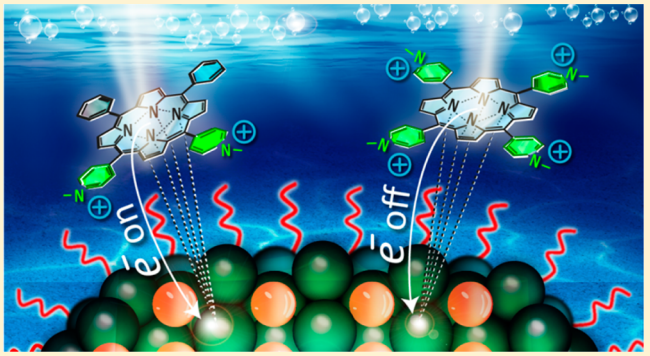

The unique electronic properties of quantum dots (QDs) have attracted widespread interest because they offer excellent platforms for the design of a new generation of bioelectronic, biosensing, and photovoltaic devices.[1−6] Additionally, the porphyrin family of compounds has been central to studies of organic solar cells due to their remarkable photoelectrochemical properties, and they have recently received very special interest in the photovoltaic community.[7−13] The electrostatic or covalent combination of porphyrins and QDs produces unique nanoassemblies with many potential applications.[14,15] Although there is a huge number of reports on the interactions of porphyrins with nanostructured materials such as gold nanoparticles,[16] silver nanospheres,[17] semiconductor QDs,[7,8,18] metal oxide nanoparticles,[19] and graphene[20,21] that have aimed to distinguish and decipher the photoinduced electron transfer (ET) from energy transfer in these porphyrin nanoassemblies, to our knowledge, no progress has been made on using molecular structure control to turn on/off the ET process at the porphyrin−nanostructure interface.

In this Letter, using the state-of-the-art time-resolved laser spectroscopy with broad-band capabilities, we present the first report of on/off ET control between water-soluble thioglycolic acid (TGA)-capped CdTe QDs and four charged porphyrins: *meso*-tetra(*N*-methyl-4-pyridyl)porphine tetrachloride (TMPyP), 5,10,15-tri(*N*-methyl-4-pyridyl)-20-(4-pyridyl)-porphine trichloride (tri-MPyP), *meso*-*cis*-di(*N*-methyl-4-pyridyl)diphenyl porphine dichloride (*cis*-diMPyP), and 5,15-diphenyl-10,20-di(*N*-methyl-4-pyridyl)porphine dichloride (*trans*-diMPyP). In these systems, switching between ET and intersystem crossing (ISC) is found to be possible by controlling the number and location of the positively charged pyridinium groups on the meso positions of the porphyrin macrocycles (see Figure 1 and Scheme 1, Supporting Information). For the TMPyP− and tri-MPyP−CdTe QD nanoassemblies, only ISC is observed. In sharp contrast, ultrafast electron injection from diMPyP to the QDs is evident for the *cis*-diMPyP−CdTe QD assembly. In addition, our time-

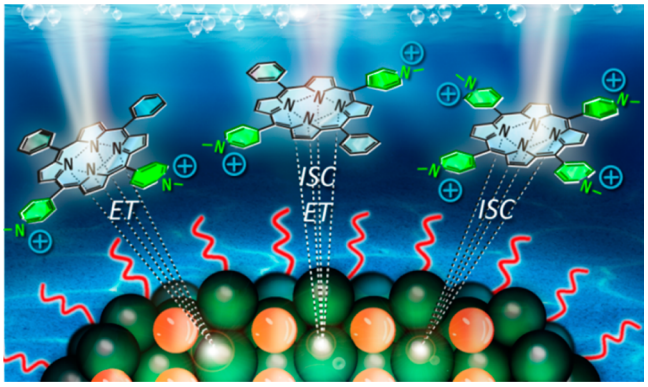

Figure 1. Different interaction mechanisms at the interface of porphyrin−CdTe QD assemblies, as tailored by the number and position of positively charged substituents.

Received: February 3, 2015
Accepted: February 11, 2015
Published: February 11, 2015

DOI: 10.1021/acs.jpclett.5b00235
J. Phys. Chem. Lett. 2015, 6, 791−795

resolved data indicate that a combination of ISC and ET processes are responsible for the excited-state deactivation of *trans*-diMPyP in its nanoassembly with CdTe QDs.

As shown in Figure 2, all of the free porphyrins exhibit the intense Soret band (S_0-S_2) at ~420 nm together with the four

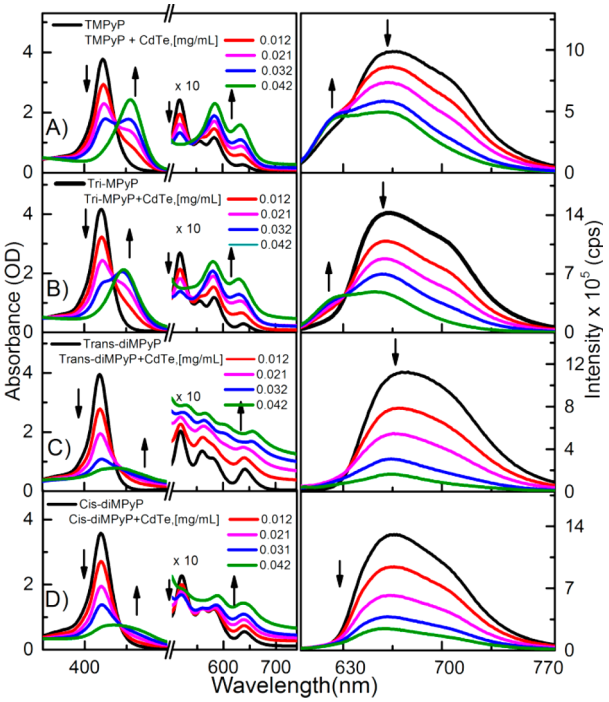

Figure 2. Absorption (left) and emission (right, $\lambda_{exc.}$ = 550 nm) of (A) TMPyP, (B) tri-MPyP, (C) *trans*-diMPyP, and (D) *cis*-diMPyP with successive additions of CdTe QDs.

Q-bands (S_0-S_1) over the range of 515−670 nm. For both TMPyP and tri-MPyP, the addition of CdTe QDs results in a decrease of the initial Soret band absorption intensity accompanied by the appearance of a new ~30 nm red-shifted spectral feature. Moreover, the number of Q-bands is reduced from four to two bands, providing a clear indication of the change in symmetry of the porphyrin macrocycle, that is, a metalation-like structure is produced.[22] Accordingly, the macrocycle for these two porphyrins adopts the out-of-plane or sitting-atop (SAT) configurations associated with assembly formation outside of the macrocyclic cavity.[19] On the other hand, for *trans*-diMPyP and *cis*-diMPyP, in addition to a weak shoulder observed at ~450 nm, a new broad-band feature appears in the 515−700 nm spectral range. These bands are characteristic of the formation of a ground-state CT complex between porphyrins and QDs.[23−25] It is worth mentioning here that Q-bands of these porphyrins still exhibit the same vibronic features of the free porphyrin after the addition of the QDs, which indicates no change in the symmetry, contrary to the TMPyP and tri-MPyP. The steady-state emission recorded after porphyrin-selective excitation at 550 nm is displayed in Figure 2, which shows strong fluorescence quenching upon the addition of CdTe QDs. It is worth mentioning that fluorescence quenching may also be achieved by energy transfer, but this mechanism can be ruled out due to the lack of spectral overlap between the absorption of CdTe QDs and the emission of the porphyrins (see Figure S1, Supporting Information). In addition, on the basis of the results of control experiments conducted at low porphyrin concentration (see Figure S2, Supporting Information), we can exclude the possibility of porphyrin aggregation.

As shown in Figure 2, a blue-shifted emission band appears upon the addition of CdTe QDs to TMPyP and tri-MPyP. This confirms that the SAT configuration of these porphyrins on the surface of the QDs is facilitated by the cross talk between the positive charge on the methylpyridinium ($^+N-CH_3$) meso units of the porphyrin and the negatively charged TGA groups capping the surface of the CdTe QDs. In this configuration, the energy gap between the highest occupied molecular orbital (HOMO) and the lowest unoccupied molecular orbital (LUMO) is increased compared with that for the free-base porphyrin.[26] Hence, the observed quenching can be attributed to an increase in the rate of singlet-to-triplet ISC by virtue of the heavy atom effect associated with Cd^{2+} on the QD surface.[27] The new blue-shifted band is very small in the case of *cis*-diMPyP, for which only strong fluorescence quenching is observed. To understand the difference in the interaction for the case of *cis*-diMPyP, we need to consider the difference in the number and position of the $^+N-CH_3$ meso units. It is known that the electron−acceptor properties of $^+N-CH_3$ substituents on TMPyP will dissipate electron density from the porphyrin macrocycle via intramolecular CT.[28] Hence, decreasing the number of these EA units will localize the electron density on the porphyrin macrocycle, and consequently, different modes of interaction are anticipated.

It should be noted that *trans*-diMPyP might have similar charge localization on the macrocycle. However, on the basis of the location of the two cationic meso units in *trans*-diMPyP, the interaction with the QD surface is expected to be different compared with that of *cis*-diMPyP. These different modes of interaction are confirmed by Raman spectra measured for the porphyrins with and without the addition of CdTe QDs (see Figure 3). It is worth pointing out that the surface coverage of

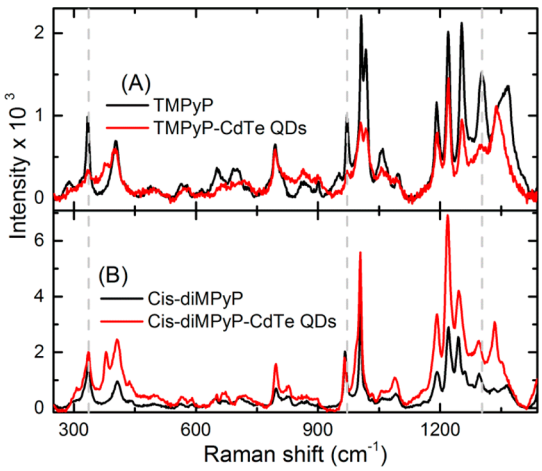

Figure 3. Raman spectra of (A) TMPyP and TMPyP−CdTe QDs and (B) *cis*-diMPyP and *cis*-diMPyP−CdTe QDs.

porphyrin units on QDs has been estimated from the effective diameter of TMPyP as ~2 nm,[25] and the approximate radius of the QDs is ~2.8 nm. Accordingly, eight molecules of TMPyP are accommodated on single QDs.

For the TMPyP−CdTe QD assemblies, the disappearance of the peaks corresponding to the in-plane bending mode at 335 cm^{-1},[19,29] the in-plane bending of pyridine at 970 cm^{-1}, and the

DOI: 10.1021/acs.jpclett.5b00235
J. Phys. Chem. Lett. 2015, 6, 791−795

free-base TMPyP macrocycle moiety at 1300 cm^{-1} indicates the formation of a metalation-like structure in the nanoassembly.[19,29] On the other hand, for *cis*-diMPyP, only an overall enhancement of the Raman spectra recorded for the free porphyrin is observed for the corresponding QD nanoassembly, which is attributed to CT complex formation at the porphyrin−QD interface.[25]

We mention here that we ruled out metalation with free Cd^{2+} ions given the following evidences: (1) The lack of interaction between neutral 5,10,15,20-tetra(4-pyridyl)porphyrin (TPyP) and CdTe QDs, as shown in Figure S3 (Supporting Information). The TPyP is accessible for metal interaction, but we did not detect or observe such an interaction. (2) The steady-state absorption and emission spectra of porphyrin metalated by cadmium chloride and porphyrin on the surface of the CdTe QDs show clear differences in both energy position and spectral shape (Figure S4, Supporting Information). (3) The nanosecond transient absorption (TA) and lifetime of the triplet state shown in Figures S5 and S6 (Supporting Information) exhibit a larger red shift as well as a longer triplet state lifetime induced by the QD compared with Cd^{2+}. (4) Additional experimental evidence of the effect of QD size on the triplet lifetime is shown in Figure S7 (Supporting Information), where a longer triplet lifetime is evident for nanoassemblies formed with smaller size QDs. (5) Finally, several previous studies addressed the interaction in porphyrin−CdTe QD nanoassemblies and reported no observations of the presence of Cd^{2+}-free ions in solution.[8,10,14,30−34]

Because TA provides detailed information about excited-state deactivation mechanisms including CT, ISC, and charge recombination (CR),[35−38] we performed femtosecond TA spectroscopy after porphyrin-selective excitation at 650 nm, which corresponds to the last vibronic band in the Q-band's absorption of the porphyrins while far from the QD confinement band (see Figure S1, Supporting Information); the resulting TA spectra with and without CdTe QDs are displayed in Figure 4, and kinetic traces are presented in Figure 5. For all of the free porphyrins, the TA spectra show similarity and agreement with those reported in the literature.[39,40] The TA spectra of TMPyP and tri-MPyP with and without CdTe QDs exhibit the same features, and no signature of the ET is observed (see Figure 4A and B).

However, a clear spectral shift is recorded and can be associated with the suggested SAT configuration adopted by the porphyrin on the surface of the QDs,[27,41,42] On the other hand, the di-($^{+}N-CH_3$) substituted porphyrins interacted differently with CdTe QDs, as indicated from the steady-state experiments and TA spectra (see Figure 4C and D). For *trans*-diMPyP, a spectral feature at 550 nm overlapping with transient features of the free porphyrin is observed but decays quickly and ends up with the TA spectra of the excited state of the free porphyrin. This new feature at 550 nm is attributed to a porphyrin cation radical[43,44] resulting from ET from the porphyrin to the CdTe QDs. However, the residual free porphyrin spectral signature at long delays indicates that the ET process is not very efficient at deactivating the excited state. The kinetic profiles monitored at two different wavelengths, 398 nm (excited-state absorption) and 550 nm (radical cation absorption), are given in Figure 5.

The decay profile at 550 nm was fit to a double-exponential decay function, which has a fast component of 11.7 ± 2.6 ps and a slow component of ∼420 ± 29 ps. The short-lived component can be assigned to CR following the ultrafast ET

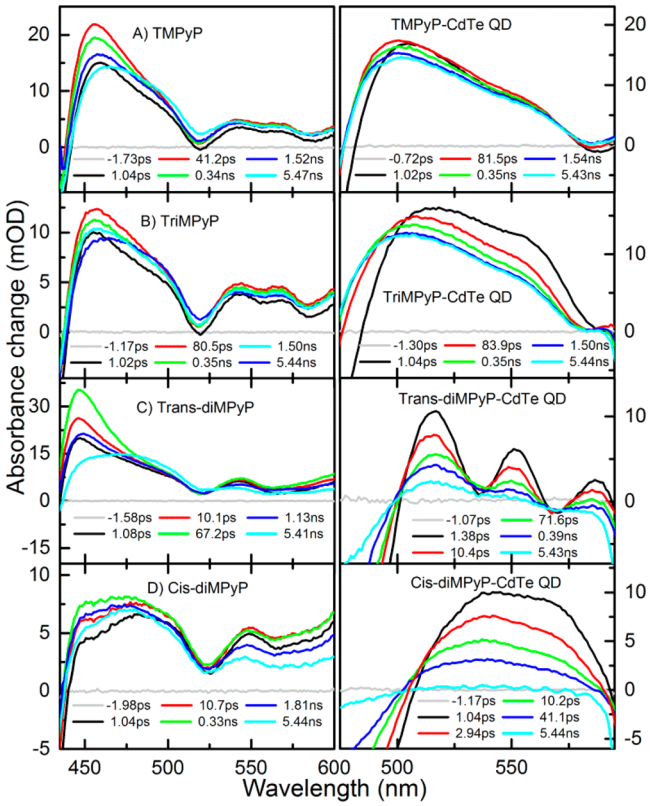

Figure 4. TA spectra ($\lambda_{exc.}$ = 650 nm) of (A) TMPyP, (B) tri-MPyP, (C) *trans*-diMPyP, and (D) *cis*-diMPyP (left) and their corresponding nanoassemblies with CdTe QDs (right).

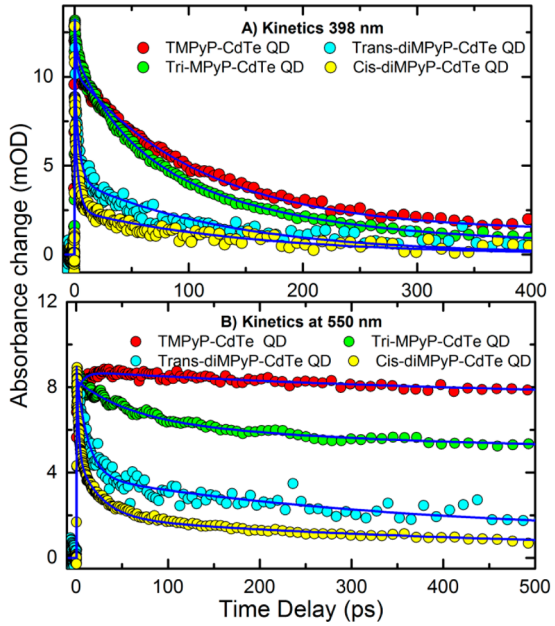

Figure 5. Kinetic traces of porphyrin−QD assemblies ($\lambda_{exc.}$ = 650 nm) collected at (A) 398 and (B) 550 nm of TMPyP (red), tri-MPyP (green), *trans*-diMPyP (cyan), and *cis*-diMPyP (yellow). The solid blue lines are the corresponding fits.

from the porphyrins to the CdTe QDs, while the long-lived component may be attributed to ISC of the porphyrins that did not undergo ET. On the other hand, the *cis*-diMPyP−CdTe QD assembly shows only a broad-band feature over the 500−

DOI: 10.1021/acs.jpclett.5b00235
J. Phys. Chem. Lett. 2015, 6, 791−795

600 nm spectral range formed within 120 fs, which is our temporal resolution. Again, this band can be safely assigned to the radical cation of the porphyrin.[43,44] The kinetic trace collected here is dominated by CR with characteristic time constants of a few and tens of ps. Importantly, the complete disappearance of the free porphyrin TA in the case of *cis*-diMPyP, while being detected for *trans*-diMPyP, indicates that the ET for the cis isomer is more efficient.

Further confirmation of the above suggested mechanisms (see eqs 1 and 2) came from the nanosecond TA spectra collected following 650 nm excitation (see Figure S8, Supporting Information)

$$\text{TMPyP}-\text{CdTe (QD)} \xrightarrow[(650\ \text{nm})]{h\nu} {}^{1}\text{TMPyP}^{*}-\text{CdTe (QD)} \xrightarrow{\text{ISC}} {}^{3}\text{TMPyP}^{*}-\text{CdTe (QD)} \quad (1)$$

$$\textit{cis}\text{-diMPyP}-\text{CdTe (QD)} \xrightarrow[(650\ \text{nm})]{h\nu} {}^{1}\textit{cis}\text{-diMPyP}^{*}-\text{CdTe (QD)} \xrightarrow{\text{ET}} {}^{1}\textit{cis}\text{-diMPyP}^{\bullet+}-\text{CdTe}^{\bullet-}\text{ (QD)} \quad (2)$$

The obtained TA spectra agree in terms of shape, peak location, and lifetime with the triplet−triplet absorption of the free porphyrins.[45,46] As can be seen in Figures S8 and S9 (Supporting Information), there are two major differences between the nanosecond TA spectra of free TMPyP and that of its QD assembly. The first is the red shift of the high-energy absorption band in the nanoassembly, which is consistent with the change in configuration discussed above. The second difference is the longer triplet-state lifetime, as indicated by the kinetic trace displayed in Figure S9A (Supporting Information). The suggested SAT configuration adopted by the porphyrin on the QD surface most likely introduces some extra restrictions on the rotation of the meso group together with increased ISC by adopting the metalated porphyrin symmetry. On the other hand, the TA spectra collected for the *trans*-diMPyP−CdTe nanoassembly shown in Figure S8B (Supporting Information) also exhibit the triplet−triplet absorption. This observation together with the femtosecond TA data suggests that both ET and ISC participate in the excited-state deactivation. In contrast, as shown in Figure S8 (Supporting Information), the *cis*-diMPyP−CdTe nanoassembly exhibits a very weak feature, and the extracted kinetic trace displayed in Figure S9 (Supporting Information) shows a very short lifetime (likely associated with CR of separated ions) compared with that of free *cis*-diMPyP. Accordingly, ET in the singlet state is the dominant process for the deactivation of the excited state.

In summary, several studies using various state-of-the-art experimental techniques and computational methods have been performed not only to access, evaluate, and provide new insights into the rate of the ET and CR at donor−acceptor interfaces but also to link such fundamental dynamical processes to practical photovoltaic device studies. However, to our knowledge, using molecular structure control to turn on/off the ET process at D/A interface is a research direction that has, until now, seen no progress. Here, we have reported the first experimental observations of controlled on/off ultrafast electron injection using cationic porphyrin−CdTe QD nanoassemblies as a unique model system. Our results clearly demonstrate the possibility of modulating the ET process at the porphyrin−CdTe QD interface. It can be tuned from zero to very efficient and ultrafast by controlling the charge localization of the porphyrin macrocycle, the number of positively charged meso units, and the magnitude of the electrostatic interaction between the positively charged meso units and the carboxylic groups of the ligand coating the QD. Finally, the novel insights reported in this study provide an understanding of the key variables involved in the nanoassembly, thus paving the way toward the exploitation of efficient ET at D/A interfaces, which is the key element and urgently required for optimal device performance.

■ ASSOCIATED CONTENT

Supporting Information

Experimental setup, sample preparation and methods, as well as some steady-state transient absorption and the kinetic profile are included. This material is available free of charge via the Internet at http://pubs.acs.org.

■ AUTHOR INFORMATION

Corresponding Author

*E-mail: omar.abdelsaboor@kaust.edu.sa.

Notes

The authors declare no competing financial interest.

[†]S.M.A.: On leave from Chemistry Department, Assiut University, Egypt.

■ ACKNOWLEDGMENTS

S.M.A. is grateful for the postdoctoral fellowship provided by SABIC. The work reported here was supported by the King Abdullah University of Science and Technology.

■ REFERENCES

(1) Kamat, P. V.; Tvrdy, K.; Baker, D. R.; Radich, J. G. Beyond Photovoltaics: Semiconductor Nanoarchitectures for Liquid-Junction Solar Cells. *Chem. Rev.* **2010**, *110*, 6664−6688.

(2) Kamat, P. V. Quantum Dot Solar Cells. The Next Big Thing in Photovoltaics. *J. Phys. Chem. Lett.* **2013**, *4* (6), 908−918.

(3) Nozik, A. J. Quantum Dot Solar Cells. *Phys. E* **2002**, *14* (1−2), 115−120.

(4) Meng, F.; Zhong, Z. Polymersomes Spanning from Nano- to Microscales: Advanced Vehicles for Controlled Drug Delivery and Robust Vesicles for Virus and Cell Mimicking. *J. Phys. Chem. Lett.* **2011**, *2* (13), 1533−1539.

(5) Gunes, S.; Fritz, K. P.; Neugebauer, H.; Sariciftci, N. S.; Kumar, S.; Scholes, G. D. Hybrid Solar Cells Using PbS Nanoparticles. *Sol. Energy Mater. Sol. Cells.* **2007**, *91* (5), 420−423.

(6) Fleming, G. R.; Scholes, G. D.; Cheng, Y.-C. Quantum Effects in Biology. *Procedia Chem.* **2011**, *3* (1), 38−57.

(7) Jagadeeswari, S.; Paramaguru, G.; Renganathan, R. Synthesis and Characterization of Free Base and Metal Porphyrins and their Interaction with CdTe QDs. *J. Photochem. Photobiol., A* **2014**, *276*, 104−112.

(8) Jhonsi, M. A.; Renganathan, R. Investigations on the Photo-induced Interaction of Water Soluble Thioglycolic Acid (TGA) Capped CdTe Quantum Dots with Certain Porphyrins. *J. Colloid Interface Sci.* **2010**, *344*, 596−602.

(9) Kang, S.; Yasuda, M.; Miyasaka, H.; Hayashi, H.; Kawasaki, M.; Umeyama, T.; Matano, Y.; Yoshida, K.; Isoda, S.; Imahori, H. Light Harvesting and Energy Transfer in Multiporphyrin-Modified CdSe Nanoparticles. *Chem. Sus. Chem.* **2008**, *1* (3), 254−261.

(10) Keane, P. M.; Gallagher, S. A.; Magno, L. M.; Leising, M. J.; Clark, I. P.; Greetham, G. M.; Towrie, M.; Gun'ko, Y. K.; Kelly, J. M.; Quinn, S. J. Photophysical Studies of CdTe Quantum Dots in the Presence of a Zinc Cationic Porphyrin. *Dalton Trans.* **2012**, *41* (42), 13159−13166.

DOI: 10.1021/acs.jpclett.5b00235
J. Phys. Chem. Lett. 2015, 6, 791−795

(11) Vaishnavi, E.; Renganathan, R. "Turn-On-Off-On" Fluorescence Switching of Quantum Dots−Cationic Porphyrin Nanohybrid: A Sensor for DNA. *Analyst* **2014**, *139* (1), 225−234.
(12) Zenkevich, E.; Blaudeck, T.; Abdel-Mottaleb, M.; Cichos, F.; Shulga, A.; von Borczyskowski, C. Photophysical Properties of Self-Aggregated Porphyrin: Semiconductor Nanoassemblies. *Int. J. Photoenergy* **2006**, 1−7.
(13) Aly, S. M.; Goswami, S.; Alsulami, Q. A.; Schanze, K. S.; Mohammed, O. F. Ultrafast Photoinduced Electron Transfer in a π-Conjugated Oligomer/Porphyrin Complex. *J. Phys. Chem. Lett.* **2014**, *5* (19), 3386−3390.
(14) Ju, H.; Zhang, X.; Wang, J. *NanoBiosensing Principles, Development and Application*; Springer: New York, 2011.
(15) Choi, H.; Kamat, P. V. CdS Nanowire Solar Cells: Dual Role of Squaraine Dye as a Sensitizer and a Hole Transporter. *J. Phys. Chem. Lett.* **2013**, *4* (22), 3983−3991.
(16) Kotiaho, A.; Lahtinen, R.; Lehtivuori, H.; Tkachenko, N. V.; Lemmetyinen, H. Photoinduced Energy and Charge Transfer in Layered Porphyrin−Gold Nanoparticle Thin Films. *J. Phys. Chem. C* **2008**, *112*, 10316−10322.
(17) Imahori, H.; Kashiwagi, Y.; Hanada, T.; Endo, Y.; Nishimura, Y.; Yamazaki, I.; Fukuzumi, S. Metal and Size Effects on Structures and Photophysical Properties of Porphyrin-Modified Metal Nanoclusters. *J. Mater. Chem.* **2003**, *13* (12), 2890−2898.
(18) Zhang, X.; Liu, Z.; Ma, L.; Hossu, M.; Chen, W. Interaction of Porphyrins with CdTe Quantum Dots. *Nanotechnology* **2011**, *22*, 195501.
(19) Gale, P. A.; Busschaert, N.; Haynes, C. J. E.; Karagiannidis, L. E.; Kirby, I. L. Anion Receptor Chemistry: Highlights from 2011 and 2012. *Chem. Soc. Rev.* **2014**, *43* (1), 205−241.
(20) Aly, S. M.; Parida, M. R.; Alarousu, E.; Mohammed, O. F. Ultrafast Electron Injection at the Cationic Porphyrin−Graphene Interface Assisted by Molecular Flattening. *Chem. Commun.* **2014**, *50*, 10452−10455.
(21) Kamat, P. V. Graphene-Based Nanoassemblies for Energy Conversion. *J. Phys. Chem. Lett.* **2011**, *2* (3), 242−251.
(22) Gouterman, M. Study of the Effects of Substitution on the Absorption Spectra of Porphin. *J. Chem. Phys.* **1959**, *30* (5), 1139−1161.
(23) Imahori, H.; Tkachenko, N. V.; Vehmanen, V.; Tamaki, K.; Lemmetyinen, H.; Sakata, Y.; Fukuzumi, S. An Extremely Small Reorganization Energy of Electron Transfer in Porphyrin−Fullerene Dyad. *J. Phys. Chem. A* **2001**, *105*, 1750−1756.
(24) Imahori, H.; Fujimoto, A.; Kang, S.; Hotta, H.; Yoshida, K.; Umeyama, T.; Matano, Y.; Isoda, S.; Isosomppi, M.; Tkachenko, N. V.; Lemmetyinen, H. Host−Guest Interactions in the Supramolecular Incorporation of Fullerenes into Tailored Holes on Porphyrin-Modified Gold Nanoparticles in Molecular Photovoltaics. *Chem.—Eur. J.* **2005**, *11* (24), 7265−7275.
(25) Murphy, S.; Huang, L.; Kamat, P. V. Charge-Transfer Complexation and Excited-State Interactions in Porphyrin−Silver Nanoparticle Hybrid Structures. *J. Phys. Chem. C* **2011**, *115*, 22761−22769.
(26) Horváth, O.; Huszánk, R.; Valicsek, Z.; Lendvay, G. Photophysics and Photochemistry of Kinetically Labile, Water-Soluble Porphyrin Complexes. *Coord. Chem. Rev.* **2006**, *250* (13−14), 1792−1803.
(27) Harriman, A. Luminescence of Porphyrins and Metalloporphyrins. Part 3. Heavy-Atom Effects. *J. Chem. Soc., Faraday Trans. 2* **1981**, *77* (7), 1281−1291.
(28) Vergeldt, F. J.; Koehorst, R. B. M.; van Hoek, A.; Schaafsma, T. J. Intramolecular Interactions in the Ground and Excited States of Tetrakis(*N*-methylpyridyl)porphyrins. *J. Phys. Chem.* **1995**, *99* (13), 4397−4405.
(29) Blom, N.; Odo, J.; Nakamoto, K.; Strommen, D. P. Resonance Raman Studies of Metal Tetrakis(4-*N*-methylpyridyl)porphine: Band Assignments, Structure-Sensitive Bands, and Species Equilibria. *J. Phys. Chem.* **1986**, *90*, 2847−2852.
(30) De Miguel, M.; Álvaro, M.; García, H. Graphene as a Quencher of Electronic Excited States of Photochemical Probes. *Langmuir* **2012**, *28* (5), 2849−2857.
(31) Zhu, K.; Hu, X.; Ge, Q.; Sun, Q. Fluorescent Recognition of Deoxyribonucleic Acids by a Quantum Dot Meso-tetrakis(N-methylpyridinium-4-yl)porphyrin Complex Based on a Photo Induced Electron-Transfer Mechanism. *Anal. Chim. Acta* **2014**, *812*, 199−205.
(32) Bruchez, M., Jr; Moronne, M.; Gin, P.; Weiss, S.; Alivisatos, A. P. Semiconductor Nanocrystals as Fluorescent Biological Labels. *Science* **1998**, *281*, 2013−2016.
(33) Shi, L. X.; Hernandez, B.; Selke, M. Singlet Oxygen Generation from Water-Soluble Quantum Dot−Organic Dye Nanocomposites. *J. Am. Chem. Soc.* **2006**, *128* (19), 6278−6279.
(34) Zenkevich, E. I.; von Borczyskowski, C. Structure and Excited State Relaxation Dynamics in Nanoscale Self-Assembled Arrays: Multiporphyrin Complexes, Porphyrin−Quantum Dot Composites. *5th Workshop on Atomic and Molecular Physics*; 2005; Vol. *5849*, pp 29−40.
(35) Zhong, D.; Zewail, A. H. Femtosecond Dynamics of Dative Bonding: Concepts of Reversible and Dissociative Electron Transfer Reactions. *Proc. Natl. Acad. Sci. U.S.A.* **1999**, *96*, 2602−2607.
(36) El-Ballouli, A. a. O.; Alarousu, E.; Bernardi, M.; Aly, S. M.; Lagrow, A. P.; Bakr, O. M.; Mohammed, O. F. Quantum Confinement-Tunable Ultrafast Charge Transfer at the PbS Quantum Dot and Phenyl-C_{61}-butyric Acid Methyl Ester Interface. *J. Am. Chem. Soc.* **2014**, *136*, 6952−6959.
(37) Sun, J.; Yu, W.; Usman, A.; Isimjan, T. T.; Dgobbo, S.; Alarousu, E.; Takanabe, K.; Mohammed, O. F. Generation of Multiple Excitons in Ag_2S Quantum Dots: Single High-Energy versus Multiple-Photon Excitation. *J. Phys. Chem. Lett.* **2014**, *5* (4), 659−665.
(38) Chuang, C.-H.; Lo, S. S.; Scholes, G. D.; Burda, C. Charge Separation and Recombination in CdTe/CdSe Core/Shell Nanocrystals as a Function of Shell Coverage: Probing the Onset of the Quasi Type-II Regime. *J. Phys. Chem. Lett.* **2010**, *1* (17), 2530−2535.
(39) Enescu, M.; Steenkeste, K.; Tfibel, F.; Fontaine-Aupart, M.-P. Femtosecond Relaxation Processes from Upper Excited States of Tetrakis(N-methyl-4-pyridyl)porphyrins Studied by Transient Absorption Spectroscopy. *Phys. Chem. Chem. Phys.* **2002**, *4* (24), 6092−6099.
(40) Villamaina, D.; Bhosale, S. V.; Langford, S. J.; Vauthey, E. Excited-State Dynamics of Porphyrin−Naphthalenediimide−Porphyrin Triads. *Phys. Chem. Chem. Phys.* **2013**, *15* (4), 1177−1187.
(41) Rodriguez, J.; Kirmaier, C.; Holten, D. Optical Properties of Metalloporphyrin Excited States. *J. Am. Chem. Soc.* **1989**, *111* (17), 6500−6506.
(42) Borissevitch, I. E.; Gandini, S. C. M. Photophysical Studies of Excited State Characteristics of Meso-tetrakis(4-N-methylpyridiniumyl)porphyrin Bound to DNA. *J. Photochem. Photobiol., B* **1998**, *43* (2), 112−120.
(43) Wojcik, A.; Kamat, P. V. Reduced Graphene Oxide and Porphyrin. An Interactive Affair in 2-D. *ACS Nano* **2010**, *4*, 6697−6706.
(44) El-Khouly, M. E.; Ito, O.; Smith, P. M.; D'Souza, F. Intermolecular and Supramolecular Photoinduced Electron Transfer Processes of Fullerene−Porphyrin/Phthalocyanine Systems. *J. Photochem. Photobiol., C* **2004**, *5*, 79−104.
(45) Keane, P. M.; Kelly, J. M. Triplet-State Dynamics of a Metalloporphyrin Photosensitiser (PtTMPyP4) in the Presence of Halides and Purine Mononucleotides. *Photochem. Photobiol. Sci.* **2011**, *10* (10), 1578−1586.
(46) Barbosa Neto, N. M.; Correa, D. S.; De Boni, L.; Parra, G. G.; Misoguti, L.; Mendonca, C. R.; Borissevitch, I. E.; Zilio, S. C.; Goncalves, P. J. Excited States Absorption Spectra of Porphyrins — Solvent Effects. *Chem. Phys. Lett.* **2013**, *587*, 118−123.

DOI: 10.1021/acs.jpclett.5b00235
J. Phys. Chem. Lett. 2015, 6, 791−795